Lateral Proton Transfer between the Membrane and a Membrane Protein[†]

Linda Öjemyr,[‡] Tor Sandén,[§] Jerker Widengren,[§] and Peter Brzezinski*[,‡]

Department of Biochemistry and Biophysics, The Arrhenius Laboratories for Natural Sciences, Stockholm University, and Experimental Biomolecular Physics, Department of Applied Physics, Royal Institute of Technology, Albanova University Center, SE-106 91 Stockholm, Sweden

Received December 3, 2008; Revised Manuscript Received January 19, 2009

ABSTRACT: Proton transport across biological membranes is a key step of the energy conservation machinery in living organisms, and it has been proposed that the membrane itself plays an important role in this process. In the present study we have investigated the effect of incorporation of a proton transporter, cytochrome *c* oxidase, into a membrane on the protonation kinetics of a fluorescent pH-sensitive probe attached at the surface of the protein. The results show that proton transfer to the probe was slightly accelerated upon attachment at the protein surface ($\sim 7 \times 10^{10}$ s^{-1} M^{-1}, compared to the expected value of $(1-2) \times 10^{10}$ s^{-1} M^{-1}), which is presumably due to the presence of acidic/His groups in the vicinity. Upon incorporation of the protein into small unilamellar phospholipid vesicles the rate increased by more than a factor of 400 to $\sim 3 \times 10^{13}$ s^{-1} M^{-1}, which indicates that the protein-attached probe is in rapid protonic contact with the membrane surface. The results indicate that the membrane acts to accelerate proton uptake by the membrane-bound proton transporter.

One step of the energy conservation machinery in living cells commonly involves proton translocation across a membrane by proton transporters. These transporters maintain a proton electrochemical gradient utilizing free energy provided, for example, by electron transfer or light. The free energy stored in this gradient is used, e.g., for transmembrane transport, motility, or synthesis of ATP by the ATP synthase. The membrane may simply comprise a passive insulator, which separates the positively (p-side)[1] charged and the negatively (n-side) charged compartments. However, as pointed out by Williams (*1, 2*) the energy conservation efficiency may be enhanced if the protons that are released to the p-side by a proton transporter are confined to the membrane surface, reaching, e.g., the ATP synthase by means of lateral diffusion. Under the nonequilibrium situation in a living cell this mechanism could lead to a surface-to-surface ΔpH across the membrane, which would differ from that of the solutions on either side of the membrane. In other words, the chemical properties of the membrane surface would be important when considering the overall energy conservation process. A prerequisite for the mechanism outlined above is that proton transfer along the surface is faster than that between a specific protonatable site and the bulk solution surrounding the protein−membrane system. Results from numerous studies indicate that indeed the membrane is not just a barrier and the membrane surface may provide a proton link between the various membrane-embedded proteins (for review, see refs *3*−*7*).

For membrane proteins the structural components involved in surface transport are typically acidic (Asp and Glu) and His residues while for membranes one component may be the phosphate group. Results from theoretical studies indicate that if the distance between two neighboring acidic sites at the surface is <10 Å, proton transfer between these sites may be faster than that between a specific site and the bulk solution (*6, 8*). If a large number of such groups is found at a surface, proton transfer along the surface over distances of ∼1 μm may be faster than equilibration with the surrounding water solution (*3, 9*). Proton transfer along membrane surfaces is closely related to the concept of a "proton-collecting antenna" (*10*−*12*). This term refers to an assembly of negatively charged residues (Asp and Glu) and His residues, at a protein surface, that are accessible to the water solution. Such arrangements are implicated when explaining results from experimental studies showing that protons can be taken up by membrane-bound transporters at rates which exceed those of proton diffusion in water (*3, 9, 13*). The idea is that the negatively charged residues attract protons while the His residues, which have pK_a values close to the solution pH at physiological conditions, act as local buffer moieties increasing the local surface-accessible proton concentration. This scenario is supported by analysis of the surfaces of a number of membrane proteins, which showed that the average minimal distance between ionizable residues at the p-side of proton translocators was shorter than that in "non-pumps" (*3*). In principle, also the membrane surrounding a proton transporter could be part of the proton-collecting antenna, provided that there is protonic contact along the surface, connecting the membrane with the proton-input

[†] The project was supported by funding from the Center for Biomembrane Research at Stockholm University, the Knut and Alice Wallenberg Foundation, and the Swedish Research Council.

* Corresponding author. Phone: (+46)-8-163280. Fax: (+46)-8-153679. E-mail: peterb@dbb.su.se.

[‡] Stockholm University.

[§] Albanova University Center.

[1] Abbreviations: Cyt*c*O, cytochrome *c* oxidase; FCS, fluorescence correlation spectroscopy; DOPG, 1,2-dioleoyl-*sn*-glycero-3-[phospho-*rac*-(1-glycerol)]; DDM, dodecyl β-D-maltoside; SUV, small unilamellar vesicles; n-side, negative side of the membrane; p-side, positive side of the membrane.

10.1021/bi8022152 CCC: $40.75
Published on Web 01/23/2009

pathway(s) of the proton transporter (reviewed in ref *14*). As indicated above, such an arrangement would not only act to accelerate proton uptake from solution but also provide a surface-confined proton pathway between membrane-bound proteins.

In recent years a large number of experimental and theoretical studies, aimed at investigating and understanding lateral proton diffusion, have been performed (*3, 4, 6, 7, 11, 15*−*28*). In a recent study in our laboratories we used fluorescence correlation spectroscopy (FCS) (Figure 1a) to investigate the protonation dynamics of a membrane-surface-anchored protonatable fluorescent probe, fluorescein (Flu) (*29*). The results showed that a membrane surface composed of DOPG (1,2-dioleoyl-*sn*-glycero-3-[phospho-*rac*-(1-glycerol)], negatively charged lipids with a pK_a of ∼2) acts to accelerate the protonation rate of the probe. In the present study we extended this approach to include also a membrane-bound proton transporter, cytochrome *c* oxidase (Cyt*c*O) from *Rhodobacter* (*R.*) *sphaeroides*, in the membrane (*30, 31*).

Cyt*c*O catalyzes the reduction of molecular oxygen to water using electrons provided by cytochrome *c*, which binds on the p-side of the membrane. The reaction involves proton uptake from the n-side of the membrane, and it is also linked to pumping of protons from the n-side to the p-side of the membrane. The substrate and pumped protons are taken up through two proton-conducting pathways which start at the n-side surface and lead toward the interior of the Cyt*c*O (for review, see ref *32*).

To investigate whether there is rapid exchange of protons between the surface of Cyt*c*O and the membrane, we attached a fluorescein molecule to a Cys residue (Cys223) at the n-side surface of Cyt*c*O (cytochrome aa_3) from *R. sphaeroides* (*11*) (Figure 1b). This residue is located far from the proton pathways but near the protein−membrane interface. The site is surrounded by only a few carboxylates and His residues such that these residues would provide protonic contact of the probe with the surrounding surface but not act by themselves to significantly accelerate the protonation rate of the probe. We then compared the protonation rate of the probe in the presence and absence of a membrane (Figure 1b,c). The results show that the protonation rate of the fluorescein was increased by a factor of ∼400 upon incorporation of Cyt*c*O into the membrane, which indicates that the membrane surface is involved in proton uptake by the enzyme.

MATERIALS AND METHODS

Growing and Purification of CytcO. R. sphaeroides was grown in Sistrom medium, and His-tagged Cyt*c*O was purified using Ni-NTA affinity chromatography as described (*33*). Buffer was exchanged to 0.1 M HEPES (Sigma-Aldrich Chemie GmbH, Steinheim, Germany), pH 7.4, and 0.1% dodecyl β-D-maltoside (DDM) (Glycon Biochemicals, Luckenwalde, Germany) before freezing in liquid nitrogen. The enzyme was stored in −80 °C until use.

Labeling of Wild-Type CytcO with Fluorescein-5-maleimide. Cyt*c*O (10 μM) and 2 μM fluorescein-5-maleimide (Invitrogen, Carlsbad, CA) in 100 mM HEPES and 0.1% DDM at pH 6.9 were incubated for 15 min in the dark at room temperature while shaking gently. The reaction was stopped with excess β-mercaptoethanol (Sigma-Aldrich Chemie GmbH, Steinheim, Germany). Free fluorophore was removed using a PD10 column (GE Healthcare UK Limited, Little Chalf-ont, U.K.) and/or by concentration and redilution using Amicon ultracentrifugation tubes (Millipore, Billerica, MA). The buffer was exchanged to 100 mM KCl and 0.1% DDM. Analysis of the fluorescein-labeled Cyt*c*O using SDS−polyacrylamide gel electrophoresis (PAGE) was carried out as described in ref *34* and showed that the fluorescein was attached to subunit III of Cyt*c*O.

Reconstitution of Fluorescein-Labeled CytcO into Small Unilamellar Vesicles. Incorporation of fluorescein-labeled Cyt*c*O was performed using a modified protocol based on ref *35*. Briefly, chloroform was evaporated from the lipid solution under a stream of nitrogen resulting in formation of a lipid film of 1,2-dioleoyl-*sn*-glycero-3-[phospho-*rac*-(1-glycerol)] (DOPG) (Avanti Polar Lipids, Inc., Alabaster, AL). The lipid film was dissolved in 100 mM KCl and 0.2% cholate, pH 7.4, to 5.09×10^{-6} mol/mL. The solution was sonciated (Ultrasonic Processor XL2020; Heat Systems) with cycles of 30 s on and 30 s off for a time period of 2 min/mL of solution, resulting in formation of small unilamellar vesicles (SUVs) with a diameter of 30−40 nm. The sample was centrifuged for 40 min at 10000*g* to remove lipid aggregates and particles from the sonicator tip. The SUV solution was mixed 1:1 (v/v) with a solution of 0.4 μM Cyt*c*O in 100 mM KCl and 0.4% cholate at pH 7.4. Detergent was removed using Bio-Beads (Bio-Rad), in total 128 mg/mL, which is $^1/_{10}$ of the amount used in ref *35*.

DOPG SUVs Containing Free Fluorescein. Twenty-five milligrams of DOPG was dissolved in chloroform, which was evaporated under a flow of nitrogen as described above. The lipid film was dissolved in 100 mM KCl and 100 μM fluorescein (total volume 2 mL) and then sonicated until the solution was clear. The sample was centrifuged for 40 min at 10000*g* to remove lipid aggregates and particles from the sonicator tip. Excess fluorescein was removed on a PD-10 column.

Spectrofluorometer Measurements. The spectrofluorometer measurements were performed on a FluoroMax 3 spectrofluorometer (Horiba Jobin Yvon, Edison, NJ).

FCS Measurements. The sample was bubbled with CO_2-free air before starting measurements to remove traces of CO_2 and was kept in a closed container throughout the measurements. Furthermore, during the measurements CO_2-free air was blown over the sample. The pH was continuously monitored using a pH electrode (Inlab Semi-Micro; Mettler-Toledo International Inc., Columbus, OH) in combination with a pH meter (Jenway 3510; Jenway, Dunmow, U.K.). FCS measurements were performed on a home-built confocal setup, consisting of an Olympus IX-70 microscope body and a linearly polarized Ar ion laser (Siemens Laser, LGK 7812-1; Siemens, München, Germany) operated at 488 nm. The laser beam was focused by a 40×, NA 1.2, UPlanApo Olympus objective, to a beam waist with $1/e^2$ radius of ∼0.5 μm (estimated from the diffusion time of rhodamine 110 in water). Emitted fluorescence was collected by the same objective and imaged by a 150 mm achromatic lens onto a pinhole of 50 μm diameter, after recollimation split by a 50/50 beamsplitter cube, and finally detected by two avalanche photodiodes (APDs) (SPCMAQR-14/16; Perkin-Elmer Optoelectronics, Wellesley, MA). The detection volume

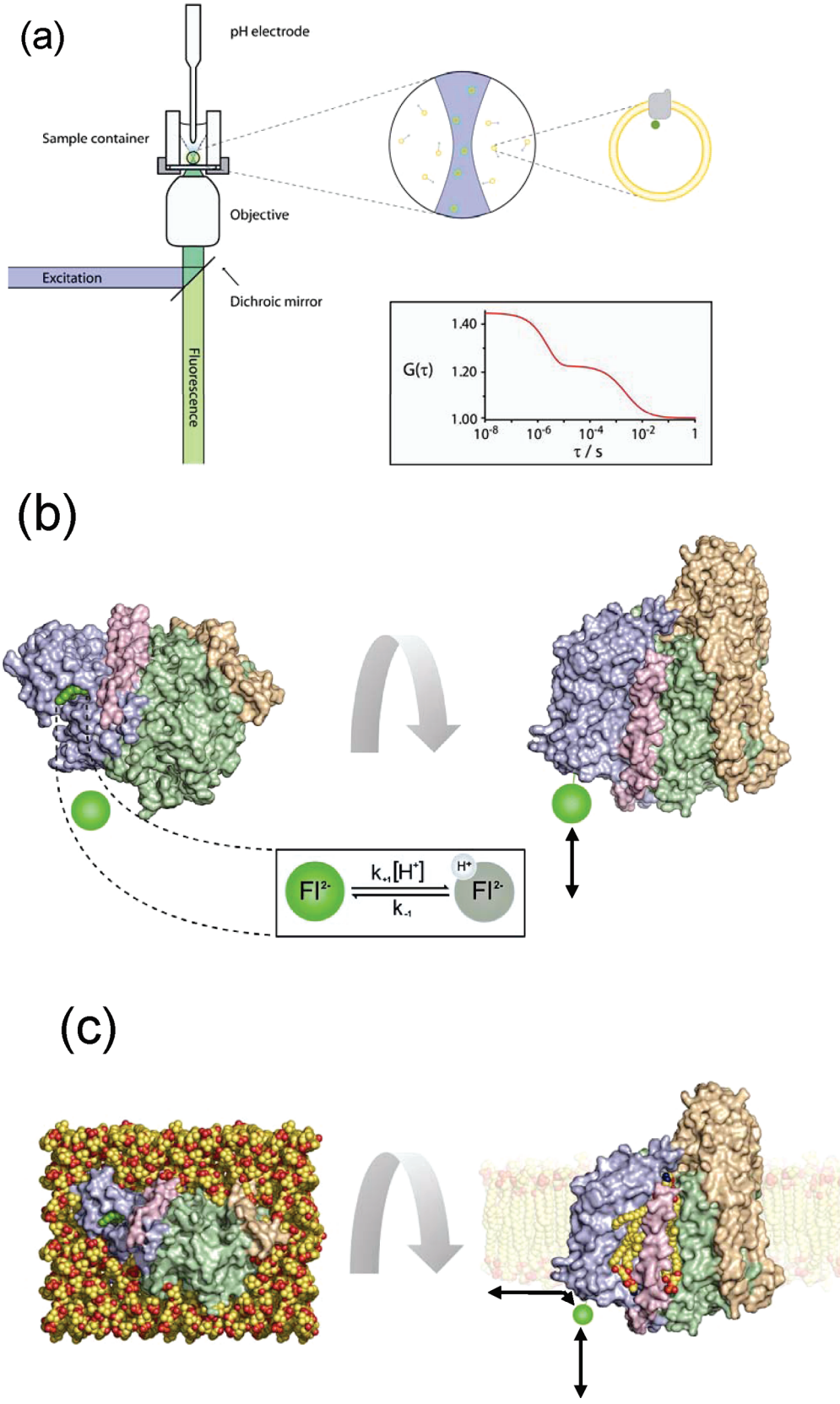

FIGURE 1: Schematic illustration of the experimental system. (a) The sample container. The fluorescein-Cyt*c*O or fluorescein-Cyt*c*O-SUVs diffuse through the detection volume (shown within the circle), and fluctuations in the fluorescence intensity are detected generating the correlation curves. The yellow circles indicate SUVs diffusing through the excitation beam in blue. (b) Cyt*c*O was labeled with a pH-sensitive fluorescein probe (green). The location of the probe (green atoms modeled into the structure of Cyt*c*O) is indicated in the structure of Cyt*c*O shown from the bottom, n-side surface, and from the side, respectively. The arrow indicates proton equilibration with the dye. Subunits I−IV of Cyt*c*O are shown in different colors (the labeled subunit III is shown in light blue). (c) Fluorescein-labeled Cyt*c*O in a membrane. The membrane is shown in yellow and red (O, P atoms). On the right-hand side (side view) the locations of lipid molecules found within the structure of the *R. sphaeroides* Cyt*c*O are indicated. The probe is found on the inside of the SUVs. The arrows indicate proton exchange with the probe (with the bulk solution and via the membrane, respectively).

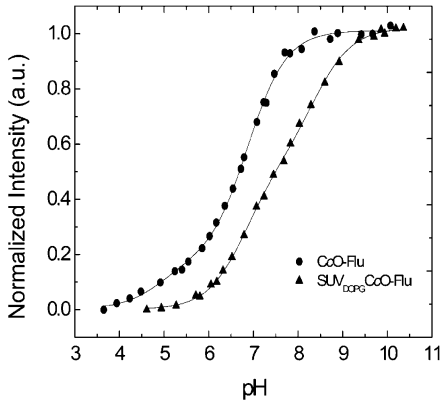

FIGURE 2: pH titration of the fluorescein fluorescence. Data are shown for the fluorescein-labeled Cyt*c*O in detergent solution (circles) and when incorporated into DOPG SUVs (triangles). Both titration curves were fitted with an equation derived from a model where the fluorescein molecule has two independently titrating protonatable groups: Cyt*c*O-fluorescein, pK_a(1) = 4.9 (17% of the total amplitude) and pK_a(2) = 6.9 (83% of the total amplitude); SUV-Cyt*c*O-fluorescein, pK_a(1) = 6.8 (52% of the total amplitude) and pK_a(2) = 8.4 (48% of the total amplitude). Experimental conditions: 100 mM KCl, 0.1% DDM (for the Cyt*c*O-fluorescein sample only), and ~22 °C.

was assumed to be a three-dimensional Gaussian with an axial $1/e^2$ extension β times (see eq 1) the transverse $1/e^2$ radius. Direct Rayleigh-scattered light from the laser beam and Raman-scattered light from the aqueous solution were suppressed by use of band-pass filters (HQ532/70; Chroma Technology Corp., Rockingham, VT) prior to fluorescence detection. The APD signals from each detector were processed by an ALV-5000/E correlator (model ALV-5000-E; ALV, Langen, Germany), with an ALV 5000/FAST Tau Extension board giving a 12.5 ns lag time resolution when cross-correlating between channels. The excitation power was kept constant (10, 30, or 75 μW yielding irradiances in the focus 1.3×10^3, 3.9×10^3, or 9.7×10^3 W/cm^2, respectively) throughout the FCS experiment. The recorded correlation curves and spectrofluorometer data were analyzed using a Levenberg−Marquardt nonlinear least-squares curve fitting algorithm (OriginPro 7.5; OriginLab, Northampton, MA).

RESULTS

Analysis of the fluorescein-labeled Cyt*c*O using SDS−PAGE showed that the probe was attached to subunit III of the *R. sphaeroides* Cyt*c*O. There is a total of three Cys residues in this subunit: Cys143, Cys146, and Cys223 (*30*). The two former residues are located close to each other (closest distance ~3.5 and ~7 Å between the sulfurs) in the interior of the protein, near the interface to the membrane, while Cys223 is located close to the n-side surface. Consequently, we assume that the fluorescein is covalently bound at Cys223. This assumption is also supported by earlier studies (*11*) and the data described below, which show that the Cyt*c*O-attached fluorescein displays characteristics similar to those of a free fluorescein in solution, indicating that the probe is bound to a residue near the protein surface (Figure 1b).

Figure 2 shows pH titrations of fluorescein covalently bound to detergent-solubilized Cyt*c*O and to Cyt*c*O incorporated into small unilamellar vesicles (SUVs) composed

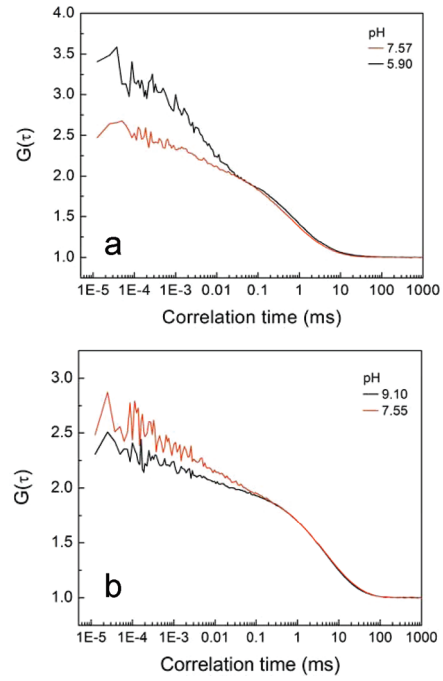

FIGURE 3: Correlation curves at two selected pH values: (a) fluorescein-labeled Cyt*c*O in detergent solution; (b) fluorescein-labeled Cyt*c*O incorporated into DOPG SUVs. Curves in (a) and (b) are normalized so that *N* (see eq 1) corresponds to approximately one. Experimental conditions: the samples were excited at 488 nm with 30 μW (3.9×10^3 W/cm^2) and 10 μW (1.3×10^3 W/cm^2), respectively. Conditions were the same as in Figure 2.

of DOPG lipids. For the fluorescein molecule attached to the detergent-solubilized enzyme two pK_as with values of ~4.9 and ~6.9 were obtained, both similar to those obtained with free fluorescein (*6, 29, 36*). The two pK_as correspond to the carboxylate (lower pK_a) and the oxyanion of the xanthene molecule, respectively (see Scheme 1 in ref *6*. When Cyt*c*O was incorporated into a lipid membrane, the pK_as of the fluorophore shifted up to ~6.8 and ~8.4, respectively, where the two pK_as most likely correspond to the same protonatable groups (where the pK_as shifted by 1.9 and 1.5 units, respectively). The different titration behavior in the absence and presence of membrane is most likely due to different chemical environments of the titrating groups resulting in different interactions upon modification of the environment. Note that the pK_a for the fluorescein attached to Cyt*c*O differs from that in ref *11* due to different experiential conditions used in that study.

Fluctuations in fluorescence of the fluorescein-Cyt*c*O were monitored by using FCS (Figure 3). Apart from a relaxation time in the millisecond time range corresponding to the average diffusion time of the labeled proteins through the detection volume (τ_D), the recorded FCS curves revealed a relaxation time in the 0.5−5 μs time range generated from the singlet−triplet transitions within the fluorophore (τ_T) (*37*) and an additional component with a relaxation time in the 50−500 μs time range (τ_X). The latter component is most likely due to photoionization of the fluorescein. None of these relaxation times did display any significant pH dependence and were all considered as independent of pH when fitting the data (see below).

Protonation and deprotonation of the pH-sensitive fluorophore, fluorescein, gave rise to fluorescence intensity

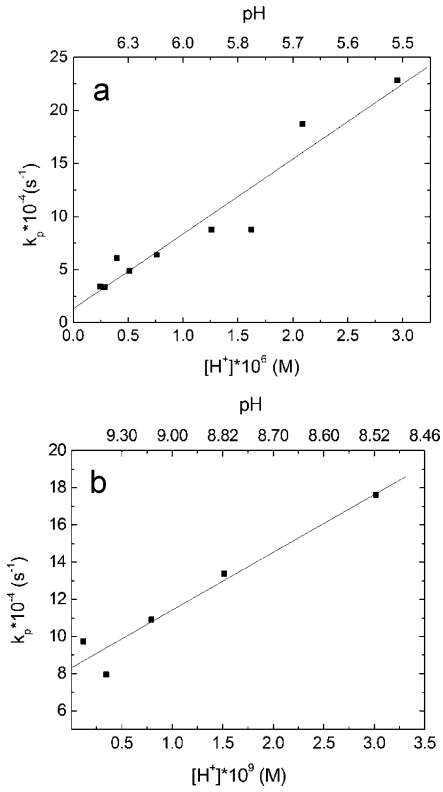

FIGURE 4: The protonation rate as a function of the proton concentration. The observed protonation rate k_P is plotted as a function of the proton concentration for fluorescein-labeled Cyt*c*O in detergent solution (a) and for fluorescein-labeled Cyt*c*O in DOPG SUVs (b). The proton on- and off-rates were extracted from the data as described in the text.

fluctuations with a relaxation time τ_P. The model used for fitting of the normalized autocorrelation curves was

$$G(\tau) = \frac{\langle F(t)F(t+\tau)\rangle}{\langle F(t)\rangle^2} = \frac{1}{N(1-T-P-X)}\left(1+\frac{\tau}{\tau_D}\right)^{-1}\left(1+\frac{\tau}{\beta^2\tau_D}\right)^{-1/2}\times (1-T-P-X+Te^{-\tau/\tau_T}+Pe^{-\tau/\tau_P}+Xe^{-\tau/\tau_X})+1 \quad (1)$$

where F signifies the detected fluorescence signal, fences denote time average, N is the average number of fluorophores in the detection volume, T is the average fraction of fluorophores residing in the triplet state, P is the fraction in the nondetected protonation state (i.e., this state gives no contribution to the signal), and X is the fraction of fluorophores in the photooxidized state.

The relaxation rate constant $k_P = 1/\tau_P$, associated with the protonation and deprotonation of fluorescein, was measured as a function of pH both for fluorescein-Cyt*c*O in detergent solution and for fluorescein-Cyt*c*O reconstituted in a membrane (Figure 4). As seen in the figure, linear dependencies were observed in both cases within the pH range covered, and the following model was used to extract the proton on, k_{+1}, and off, k_{-1}, rates:

$$k_P = k_{-1} + k_{+1}[H^+] \quad (2)$$

The data obtained with detergent-solubilized fluorescein-Cyt*c*O in the pH range 5.5−6.6 are shown in Figure 4a, and the following parameters were extracted: $k_{+1} = (7.1 \pm 0.8) \times 10^{10}$ s^{-1} M^{-1} and $k_{-1} = (1.3 \pm 1.1) \times 10^4$ s^{-1} (summarized in Table 1); i.e., the on-rate was slightly larger than that determined for free fluorescein in solution ($k_{+1} = 4.0 \times 10^{10}$ M^{-1} s^{-1}) while the off-rate was slightly lower ($k_{-1} = 2.5 \times 10^4$ s^{-1} for free fluorescein) (*36*) (similar values were also obtained using a different experimental approach (*6*)). The logarithm of the ratio of the on- and off-rates gives a pK_a of 6.7 ± 0.5, i.e., about the same as the high pK_a (6.9 ± 0.1) determined in the static titration (see Figure 2) and slightly higher than that of a free fluorescein in solution (~6.2; see Table 1).

The corresponding pK_a for the Cyt*c*O reconstituted in SUVs was found to be ~8.4. Therefore, the measurements with membrane-reconstituted Cyt*c*O were performed in the pH range 8.5−9.9 to prevent interference from the group titrating with the lower pK_a (see above). About the same pH range was used previously in experiments on model membranes (*29*). Results from measurements with fluorescein-Cyt*c*O reconstituted in DOPG lipid membranes are shown in Figure 4b. The slope of $k_P(H^+)$ increased dramatically as compared to the detergent-solubilized fluorescein-Cyt*c*O, and we obtained the following parameters: $k_{+1} = (3.1 \pm 0.4) \times 10^{13}$ s^{-1} M^{-1} and $k_{-1} = (8.3 \pm 0.7) \times 10^4$ s^{-1}. In other words, k_{+1} was more than 2 orders of magnitudes larger for the membrane-reconstituted than for the detergent-solubilized fluorescein-Cyt*c*O. The pK_a value obtained from the kinetic data, 8.6 ± 0.1, was about the same as that obtained from the static titration (see above).

To confirm that the fluorescein was still attached to the Cyt*c*O after incorporation into the membrane, we disrupted the SUVs after the FCS measurements using detergents and determined the diffusion time of the fluorophore−protein complex. This time was found to be the same as that for fluorescein-labeled Cyt*c*O and not similar to that obtained for the free fluorophore. Furthermore, we measured the pK_a (using a spectrofluorometer) for free fluorescein present in DOPG lipid vesicles and found that it displayed a value of 6.8 ± 0.1, which is somewhat higher than that of free fluorescein in water (~6.2) but significantly lower than that of fluorescein attached to a membrane (~8.5 (*29*)). These controls indicate that the fluorescein stays attached to the membrane-reconstituted Cyt*c*O throughout the measurements.

DISCUSSION

We have studied the effect of the membrane on the protonation rate of a fluorescent pH-sensitive probe, fluorescein, attached at the n-side surface of the proton transporter Cyt*c*O from *R. sphaeroides*. The probe was bound to subunit III, presumably at Cys223, which is located at a distance of ~30 Å from the nearest proton-input pathway of the Cyt*c*O (Asp132 in the D pathway). We performed these measurements with the wild-type Cyt*c*O because the putative labeling site is located relatively close to the protein−membrane interface. Furthermore, even though the site is surrounded by a few acidic and His groups (cf. components of a proton collecting antenna), these residues are relatively spread out and distantly located from the labeling site (see below). In other words, the labeled site is not surrounded by a proton-collecting antenna, and we did not expect to see any dramatic increase in the protonation rate of the Cys223-attached probe in the absence of a membrane.

Table 1: Protonation and Deprotonation Rates of Fluorescein (Flu) in Different Environments

	Flu-Cyt*c*O	Flu-Cyt*c*O-DOPG membrane	Flu-DOPG membrane[a]	Flu in water[b]
k_{+1} (M^{-1} s^{-1})	$(7.1 \pm 0.8) \times 10^{10}$	$(3.1 \pm 0.4) \times 10^{13}$	$(9.4 \pm 0.8) \times 10^{12}$	4×10^{10}
k_{-1} (s^{-1})	$(1.3 \pm 1.1) \times 10^{4}$	$(8.3 \pm 0.7) \times 10^{4}$	$(3.3 \pm 0.3) \times 10^{4}$	2.5×10^{4}
pK_a	6.7 ± 0.5 (∼6.9)[c]	8.6 ± 0.1 (∼8.4)[c]	8.5 ± 0.1 (∼8.2)[c]	6.2 (∼6.4)[c]

[a] Data from ref *29*, except the pK_a value. [b] Data from ref *36*, except the pK_a value. [c] The numbers in parentheses were determined from static titrations.

The Cys223 residue in subunit III is not fully exposed to water solution; however, it is accessible to the n-side surface through a small cavity through which the fluorescein-maleimide may enter (*30*). Furthermore, binding of the fluorescein may slightly distort the surrounding residues to accommodate the fluorophore. Because the length of the fluorescein-maleimide is ∼10 Å, the fluorescent probe itself is presumably found at the surface of the protein. That the fluorophore is accessible to water at the membrane surface is supported by the pH titration experiments, which show that its pK_a is similar to that of a free fluorescein in water solution. Furthermore, the protonation rate of the fluorescein was found to be $k_{+1} \cong 7.1 \times 10^{10}$ s^{-1} M^{-1}, i.e., larger than that for a well-exposed fluorescein attached at a surface ($(1-2) \times 10^{10}$ s^{-1} M^{-1} (*11*); this value is smaller than that for a free fluorescein in solution due to the two-dimensional nature of the surface). The observation of a slightly increased on-rate constant for the Cyt*c*O-attached fluorophore indicates that the fluorescein is accessible to the water phase and that its protonation at the surface is assisted to some extent by other protonatable groups (*10*−*12*). Inspection of the *R. sphaeroides* Cyt*c*O structure (*30*) shows that there are three separated groups of acidic and His residues located within a distance of ∼10 Å from the point at the surface where the fluorescein probe is likely to be found: (i) Glu235, (ii) Glu158, His 153, His157, and (iii) Asp163, all in subunit III. Furthermore, there is an intraprotein phosphatidylethanolamine (PE) lipid bound in the vicinity of the proposed fluorescein-binding site. Any of these groups is likely to enhance the protonation rate of the fluorescein; however, the effect is not expected to be very large as the residues are not evenly distributed but rather confined to the three clusters described above. Furthermore, none of the residues is less than 5−7 Å away from the proposed location of the fluorescein. The proton off-rate was slightly slower than that for a free fluorescein in solution, which also supports the notion that the fluorescein is deprotoned by proton transfer to an acceptor at the surface rather than spontaneous deprotonation to solution. Alternatively, the slightly higher on-rate and the lower off-rate for the protein-conjugated fluorescein, resulting in an apparent pK_a shift (see Table 1), may be due to a negative net surface charge in the local vicinity of the fluorophore, similarly to the effect observed with bacteriorhodopsin (*38*).

Incorporation of the fluorescein-labeled enzyme into DOPG SUVs resulted in an increase in the protonation on-rate by a factor of ∼400, while the off-rate increased by only a factor of ∼6. This result indicates that the increase in the pK_a upon incorporation of the fluorescein-labeled Cyt*c*O into the membrane is not simply due to a change in the probe environment because such a change would be reflected mainly in the off-rate. Furthermore, a similar increase in the protonation on-rate was observed previously upon incorporation of a fluorescein chromophore at a DOPG membrane surface (*29*). In addition, an increase in the protonation rate by a factor of 400 requires involvement of at least part of the SUV surface in proton collection (*20, 21*). In this context we note that the fluorescein pK_a value increased upon incorporation of the fluorescein-labeled Cyt*c*O into a membrane (Table 1). This change may be interpreted to reflect an increase in the surface proton concentration upon incorporation of the fluorescein-Cyt*c*O into the membrane, e.g., due to electrostatic interactions with the negatively charged phosphate groups. However, the proton activity must be the same at the surface and in solution because these systems are in equilibrium. Therefore, when comparing the protonation on-rate constants with and without a membrane, any adjustment for a putative change in the local proton concentration should not be made.

Taken together, these results indicate that the fluorescein probe at the Cyt*c*O surface is in proton equilibrium with the membrane surface. The proton connectivity between the fluorescein and the membrane surface is likely to be mediated by the acidic residue clusters at subunit III, mentioned above.

The protonation on-rate constant was a factor of ∼3 larger for the fluorescein attached to Cyt*c*O (∼3.1×10^{13} s^{-1} M^{-1}) reconstituted in a DOPG membrane than for the fluorescein alone attached to a DOPG membrane (∼9.4×10^{12} s^{-1} M^{-1}). A similar difference was observed for the off-rates leading to about the same pK_as in the two cases. These differences are presumably in part due to the different salt concentrations used in these studies, but they may also reflect small changes in the Cyt*c*O structure at the protein−membrane interface. Similarly, variations in local structure most likely also explain the difference in the off-rates measured for the membrane fluorescein-Cyt*c*O system as compared to fluorescein alone in a membrane (see Table 1).

The use of eq 2 to derive the on- and off-rate constants implicitly assumes interactions between freely diffusing (random Brownian diffusion) protons and the fluorescein molecule. This assumption is sufficient to determine the difference in the second-order protonation on-rate constants for the detergent-solubilized and membrane-reconstituted fluorescein-Cyt*c*O. However, it should be noted that the rate constants are apparent values because the protonation reaction also involves protons that are transiently bound to other surface groups (*39*). Furthermore, proton transfer along the surface most likely takes place in a heterogeneous environment where protons are transferred through transiently formed chains of water molecules ordered by short-lived interactions with the membrane and protein surfaces (*40*).

In conclusion, we have shown that the protonation rate of a protonatable probe attached to the surface of a membrane-bound protein increases dramatically upon incorporation of the protein into the membrane. The results indicate that the protein surface is in protonic contact with the membrane surface, which suggests that the membrane can provide a

pathway for proton transfer between proton transporters and proton "consumers" in the living cell.

ACKNOWLEDGMENT

We thank Dr. Nikolai Kocherginsky for valuable comments.

REFERENCES

1. Williams, R. J. P. (1978) The multifarious couplings of energy transduction. *Biochim. Biophys. Acta 505*, 1–44.
2. Williams, R. J. P. (1961) Possible functions of chains of catalysts. *J. Theor. Biol. 1*, 1–17.
3. Mulkidjanian, A. Y., Heberle, J., and Cherepanov, D. A. (2006) Protons at interfaces: Implications for biological energy conversion. *Biochim. Biophys. Acta 1757*, 913–930.
4. Heberle, J. (2000) Proton transfer reactions across bacteriorhodopsin and along the membrane. *Biochim. Biophys. Acta 1458*, 135–147.
5. Ädelroth, P., and Brzezinski, P. (2004) Surface-mediated proton-transfer reactions in membrane-bound proteins. *Biochim. Biophys. Acta 1655*, 102–115.
6. Sacks, V., Marantz, Y., Aagaard, A., Checover, S., Nachliel, E., and Gutman, M. (1998) The dynamic feature of the proton collecting antenna of a protein surface. *Biochim. Biophys. Acta 1365*, 232–240.
7. Kocherginsky, N. (2008) Acidic lipids, H^+-ATPases, and mechanism of oxidative phosphorylation. Physico-chemical ideas 30 years after P. Mitchell's Nobel Prize award, *Prog. Biophys. Mol. Biol.* (doi:10.1016/j.pbiomolbio.2008.10.013).
8. Friedman, R., Nachliel, E., and Gutman, M. (2005) Application of classical molecular dynamics for evaluation of proton transfer mechanism on a protein. *Biochim. Biophys. Acta 1710*, 67–77.
9. Heberle, J., Riesle, J., Thiedemann, G., Oesterhelt, D., and Dencher, N. A. (1994) Proton migration alone the membrane-surface and retarded surface to bulk transfer. *Nature 370*, 379–382.
10. Riesle, J., Oesterhelt, D., Dencher, N. A., and Heberle, J. (1996) D38 is an essential part of the proton translocation pathway in bacteriorhodopsin. *Biochemistry 35*, 6635–6643.
11. Marantz, Y., Nachliel, E., Aagaard, A., Brzezinski, P., and Gutman, M. (1998) The proton collecting function of the inner surface of cytochrome *c* oxidase from *Rhodobacter sphaeroides*. *Proc. Natl. Acad. Sci. U.S.A. 95*, 8590–8595.
12. Checover, S., Nachliel, E., Dencher, N. A., and Gutman, M. (1997) Mechanism of proton entry into the cytoplasmic section of the proton- conducting channel of bacteriorhodopsin. *Biochemistry 36*, 13919–13928.
13. Namslauer, A., Pawate, A. S., Gennis, R. B., and Brzezinski, P. (2003) Redox-coupled proton translocation in biological systems: Proton shuttling in cytochrome *c* oxidase. *Proc. Natl. Acad. Sci. U.S.A. 100*, 15543–15547.
14. Gutman, M., and Nachliel, E. (1995) The dynamics of proton-exchange between bulk and surface groups. *Biochim. Biophys. Acta 1231*, 123–138.
15. Antonenko, Y. N., and Pohl, P. (2008) Microinjection in combination with microfluorimetry to study proton diffusion along phospholipid membranes. *Eur. Biophys. J. 37*, 865–870.
16. Serowy, S., Saparov, S. M., Antonenko, Y. N., Kozlovsky, W., Hagen, V., and Pohl, P. (2003) Structural proton diffusion along lipid bilayers. *Biophys. J. 84*, 1031–1037.
17. Gopta, O. A., Cherepanov, D. A., Junge, W., and Mulkidjanian, A. Y. (1999) Proton transfer from the bulk to the bound ubiquinone Q_B of the reaction center in chromatophores of *Rhodobacter sphaeroides*: retarded conveyance by neutral water. *Proc. Natl. Acad. Sci. U.S.A. 96*, 13159–13164.
18. Cherepanov, D. A., Junge, W., and Mulkidjanian, A. Y. (2004) Proton transfer dynamics at the membrane/water interface: dependence on the fixed and mobile pH buffers, on the size and form of membrane particles, and on the interfacial potential barrier. *Biophys. J. 86*, 665–680.
19. Marantz, Y., Einarsdóttir, O., Nachliel, E., and Gutman, M. (2001) Proton-collecting properties of bovine heart cytochrome *c* oxidase: Kinetic and electrostatic analysis. *Biochemistry 40*, 15086–15097.
20. Georgievskii, Y., Medvedev, E. S., and Stuchebrukhov, A. A. (2002) Proton transport via the membrane surface. *Biophys. J. 82*, 2833–2846.
21. Georgievskii, Y., Medvedev, E. S., and Stuchebrukhov, A. A. (2002) Proton transport via coupled surface and bulk diffusion. *J. Chem. Phys. 116*, 1692–1699.
22. Smondyrev, A. M., and Voth, G. A. (2002) Molecular dynamics simulation of proton transport near the surface of a phospholipid membrane. *Biophys. J. 82*, 1460–1468.
23. Alexiev, U., Mollaaghababa, R., Scherrer, P., Khorana, H. G., and Heyn, M. P. (1995) Rapid long-range proton diffusion along the surface of the purple membrane and delayed proton-transfer into the bulk. *Proc. Natl. Acad.Sci. U.S.A. 92*, 372–376.
24. Scherrer, P., Alexiev, U., Marti, T., Khorana, H. G., and Heyn, M. P. (1994) Covalently bound pH-indicator dyes at selected extracellular or cytoplasmic sites in bacteriorhodopsin. 1. Proton migration along the surface of bacteriorhodopsin micelles and its delayed transfer from surface to bulk. *Biochemistry 33*, 13684–13692.
25. Krasinskaya, I. P., Lapin, M. V., and Yaguzhinsky, L. S. (1998) Detection of the local H^+ gradients on the internal mitochondrial membrane. *FEBS Lett. 440*, 223–225.
26. Gabriel, B., and Teissie, J. (1996) Proton long-range migration along protein monolayers and its consequences on membrane coupling. *Proc. Natl. Acad. Sci. U.S.A. 93*, 14521–14525.
27. Teissie, J. (1996) Lateral proton diffusion. *Nature 379*, 305–306.
28. Kocherginsky, N. M. (1979) Lipids as possible proton carriers from the respiratory chain to ATP-synthase, and the mechanism of oxidative phosphorylation. *Biophysika (USSR) 24*, 982–987.
29. Brändén, M., Sandén, T., Brzezinski, P., and Widengren, J. (2006) Localized proton microcircuits at the biological membrane-water interface. *Proc. Natl. Acad. Sci. U.S.A. 103*, 19766–19770.
30. Svensson-Ek, M., Abramson, J., Larsson, G., Törnroth, S., Brzezinski, P., and Iwata, S. (2002) The X-ray crystal structures of wild-type and EQ(I-286) mutant cytochrome *c* oxidases from *Rhodobacter sphaeroides*. *J. Mol. Biol. 321*, 329–339.
31. Qin, L., Hiser, C., Mulichak, A., Garavito, R. M., and Ferguson-Miller, S. (2006) Identification of conserved lipid/detergent-binding sites in a high-resolution structure of the membrane protein cytochrome c oxidase. *Proc. Natl. Acad. Sci. U.S.A. 103*, 16117–16122.
32. Brzezinski, P., and Gennis, R. B. (2008) Cytochrome *c* oxidase: exciting progress and remaining mysteries. *J. Bioenerg. Biomembr.,* 1–11.
33. Mitchell, D. M., and Gennis, R. B. (1995) Rapid purification of wildtype and mutant cytochrome *c* oxidase from *Rhodobacter sphaeroides* by Ni^{2+}-NTA affinity chromatography. *FEBS Lett. 368*, 148–150.
34. Varanasi, L., Mills, D., Murphree, A., Gray, J., Purser, C., Baker, R., and Hosler, J. (2006) Altering conserved lipid binding sites in cytochrome *c* oxidase of *Rhodobacter sphaeroides* perturbs the interaction between subunits I and III and promotes suicide inactivation of the enzyme. *Biochemistry 45*, 14896–14907.
35. Faxén, K., Gilderson, G., Ädelroth, P., and Brzezinski, P. (2005) A mechanistic principle for proton pumping by cytochrome *c* oxidase. *Nature 437*, 286–289.
36. Widengren, J., Terry, B., and Rigler, R. (1999) Protonation kinetics of GFP and FITC investigated by FCS—Aspects of the use of fluorescent indicators for measuring pH. *Chem. Phys. 249*, 259–271.
37. Widengren, J., Mets, U., and Rigler, R. (1995) Fluorescence correlation spectroscopy of triplet states in solution: A theoretical and experimental study. *J. Phys. Chem. 99*, 13368–13379.
38. Alexiev, U., Marti, T., Heyn, M. P., Khorana, H. G., and Scherrer, P. (1994) Surface charge of bacteriorhodopsin detected with covalently bound pH indicators at selected extracellular and cytoplasmic sites. *Biochemistry 33*, 298–306.
39. Friedman, R., Nachliel, E., and Gutman, M. (2005) Molecular dynamics of a protein surface: Ion-residues interactions. *Biophys. J. 89*, 768–781.
40. Friedman, R., Fischer, S., Nachliel, E., Scheiner, S., and Gutman, M. (2007) Minimum energy pathways for proton transfer between adjacent sites exposed to water. *J. Phys. Chem. B 111*, 6059–6070.

BI8022152